Nanoscale

PAPER

View Article Online
View Journal | View Issue



Cite this: *Nanoscale*, 2022, **14**, 5840

# Robust multifunctional fluorine-free superhydrophobic fabrics for high-efficiency oil–water separation with ultrahigh flux†

Zheng Xiong,[a] Jian Huang,*[a] Yongzhong Wu[b] and Xiao Gong *[a]

Received 18th January 2022,
Accepted 7th March 2022

DOI: 10.1039/d2nr00337f

rsc.li/nanoscale

The limited robustness and complex preparation process greatly hinder the large-scale use of superhydrophobic surfaces in real life. In this work, we adopt a simple method to prepare robust fluorine-free superhydrophobic cotton fabrics by a facile dip-coating method based on silica microparticles and titanium dioxide nanoparticles. Microparticles and nanoparticles are used to build a suitable rough hierarchical structure, while strong bonds are formed between fabric and particles by a silane coupling agent. The cross-linking reaction between the isocyanate group of trimers of hexamethylene diisocyanate (HDI) and the hydroxyl group of each component in the condensation reaction further increases the bonding between the coating and the cotton fabric. In addition, polydimethylsiloxane (PDMS) is used as a low-surface-energy material to modify the fabric surface. The resulting coating shows excellent superhydrophobic properties with a water contact angle of 161.7°. Meanwhile, the prepared superhydrophobic fabric exhibits excellent durability and stability after sandpaper wearing, washing, and UV radiation, as well as treatment with various organic solutions, boiling water and different pH solutions. Moreover, the superhydrophobic fabric displays excellent UV protection performance and high oil–water separation efficiency (>99% after 30 cycles) with ultrahigh flux up to 20 850 L $m^{-2}$ $h^{-1}$.



## 1. Introduction

Superhydrophobic surfaces with a water contact angle (WCA) larger than 150° and sliding hysteresis angle (SHA) less than 10°, play a key role in many fields due to their extremely water repellent properties such as self-cleaning,[1–5] anti-icing,[6–8] metal anti-corrosion,[9] fog harvesting,[10] marine drag reduction[11] and oil–water separation.[12–19] Through the study of the lotus leaf surface which can make raindrops roll and bounce to remove contaminants, it is found that micro–nano "papillae" structures and the waxy substance covering the surface are the main reasons for this "self-cleaning" phenomenon.[20] Furthermore, rough structure and chemical composition are highly correlated with hydrophobicity from the classical Wenzel[21] and Cassie–Baxter models.[22] According to the Wenzel model, rough structures featuring hierarchical micro–nanostructures can improve hydrophobic properties. The Cassie–Baxter model further illustrates that the rough structure can trap air to form an air cushion between water and solid surfaces, resulting in water droplets rolling off easily.

As a natural fiber, cotton fabric with low cost and high yield has been widely used in industries and households owing to comfort, softness, breathability, wash resistance and moisture absorption.[23,24] Modifying cotton fabrics to be superhydrophobic will expand their applications in oil–water separation[25–28] and self-cleaning,[29–31] thus many representative methods have emerged including, spray-coating,[32] phase separation,[33] layer-by-layer self-assembly, and chemical vapor deposition.[34] However, there are many issues in the above methods such as complicated preparation process, expensive equipment, long reaction time, and toxic fluorine-containing low-surface-energy material, restricting large-scale applications. In contrast, the dip-coating method[35–37] is a simple, time-saving and environmentally friendly preparation method of superhydrophobic materials. Pal *et al.*[38] fabricated superhydrophobic cotton by dip coating titanium dioxide sol onto the surface of cotton fabric to form a rough structure followed by hydrophobic 3-(trimethoxysilyl)propyl methacrylate surface modification. Shang *et al.*[39] used tannic acid to activate the surface of cotton fabric which was then grafted with aminopropylisobutyl polyhedral oligomeric silsesquioxane ($NH_2$-POSS) through the Schiff-base/Michael-addition reaction with a WCA of 158.6°. Chen *et al.*[40]

[a]*State Key Laboratory of Silicate Materials for Architectures, Wuhan University of Technology, Wuhan 430070, P. R. China. E-mail: JHuang@whut.edu.cn, xgong@whut.edu.cn*
[b]*School of Mechanical Engineering, Suzhou University of Science and Technology, Suzhou 215009, China*

† Electronic supplementary information (ESI) available. See DOI: https://doi.org/10.1039/d2nr00337f

prepared superhydrophobic cotton fabrics using vinyl trimethoxysilane (VTMS), resulting in more reactive vinyl, and then hydrophobically modified with mercaptan by thiol–ene click chemistry reaction. Shang *et al.*[41] also fabricated superhydrophobic/superoleophilic cotton fabrics using a novel castor oil-based thiolated oligomer, octavinyl polyhedron oligomeric sesquiloxane and hydrophobic $SiO_2$ with thiol–ene click chemistry reaction. However, the superhydrophobic cotton fabrics prepared by these methods are not resistant to wear and washing, therefore they are difficult to apply in complex and harsh environments. In addition, the development of multifunctional cotton fabrics has become a hot research topic,[41] which can meet the diverse needs of people's daily lives. In the actual application process, ultraviolet rays tend to pass through the fabric and interact with skin, accelerating skin aging and causing various diseases.[42] Therefore, it is necessary to combine the advantages of superhydrophobic cotton fabric with UV-shielding materials to form a multifunctional fabric.

Herein, a robust fluorine-free self-cleaning superhydrophobic cotton fabric is prepared by a dip-coating process, which is coated with a combination of micron-sized silica and nano-sized titanium dioxide and hydrophobically modified by polydimethylsiloxane (PDMS). The hierarchical lotus-leaf-like surface structure formed on the cotton fabric surface not only improves the roughness, but also captures air to form an air cushion between the coating and the water droplets. Furthermore, strong bonds are formed between cotton fabric and particles by the silane coupling agent, wherein the micron-sized silicon dioxide protects the nano-sized titanium dioxide from damage and makes it better able to shield UV light. The cross-linking reaction which occurs between the isocyanate group of trimers of hexamethylene diisocyanate (HDI) and the hydroxyl group of each component in the condensation reaction can further increase the bond between the superhydrophobic coating and the cotton fabric. This preparation method is simple, low-cost, efficient, and environmentally friendly due to fluorine-free substances, and the prepared superhydrophobic cotton fabric exhibits high wash resistance durability, chemical stability, strong self-cleaning performance, excellent UV shielding ability, and high oil–water separation efficiency with ultrahigh flux.

## 2. Experimental section

### 2.1 Materials

Cotton fabrics were purchased from local stores. Polydimethylsiloxane (Sylgard184) and its curing agent, Sudan IV, *N*-[3-(trimethoxysilyl)propyl]ethylenediamine (KH792) and hydrophilic silica micropowder (>99.8% metals basis, 1 μm, spherical) were provided by Aladdin. Nano-titania, dichloroethane, carbon tetrachloride and bromobenzene were supplied by Shanghai Macklin. Ethanol, dichloromethane, butyl acetate and methylene blue were provided by Sinopharm Chemical Reagent Co., Ltd. The curing agent was a trimer of hexamethylene diisocyanate (HDI) purchased as the Covestro product N3300.

### 2.2 Preparation of superhydrophobic cotton fabric

The robust superhydrophobic cotton fabric was prepared by two-step dip coating and the schematic diagram of the preparation process is shown in Scheme 1. Pristine cotton fabric was rinsed with water and ethanol three times to remove impurities on the surface. Titanium dioxide and silicon dioxide with different mass ratios were added to 63 mL of ethanol and dispersed by ultrasonication for 30 min. Then, 500 μL of KH792 was added to the above solution with magnetic stirring for 1 h. The solution prepared in this way was denoted as A. The preparation method for solution B is as follows: 1 g of PDMS and 0.1 g of its curing agent were added to 74 mL of *n*-hexane with ultrasonic dispersion for 15 min, and then 1 mL of N3300 was added and stirred for 30 min to form a stable solution. The cleaned cotton was soaked in solution A for 10 min, and then dried at room temperature. Afterwards, the dried cotton fabric was dipped in solution B for 2 min, and finally placed in a 120 °C oven to be cured for 2 h.

### 2.3 Durability and chemical stability tests

Durability tests mainly include washing, sandpaper wear and UV resistance tests. For the washing durability test modified from the literature, the superhydrophobic cotton fabric was immersed in 1 wt% detergent followed by stirring at 300 rpm for 30 min at 50 °C, which was recorded as one cycle. And the WCA was measured every 10 cycles. For the abrasion test, the cotton fabric was attached to a glass slide with double-sided tape, and then the side with the cotton surface was placed on 800/1000/2000 grit sandpaper with a 100 g weight, respectively. The sample was moved slowly at a speed of 5 cm $s^{-1}$ for 10 cm in the horizontal and vertical directions as one cycle. WCA was measured every 5 cycles. For the UV resistance test, the cotton was irradiated under a UV lamp (power: 1 kW; the cotton sample was placed 15 cm directly under the UV lamp) for 3 h as one cycle, and WCA was measured once in each cycle.

The chemical stability test was carried out by putting the superhydrophobic cotton fabrics into different extreme environments, including solutions with various pH values (1, 3, 5, 7, 9, 11, and 13), different organic solvents (*e.g.*, DMF, DMSO, acetone, *n*-hexane, toluene, ethanol) and boiling water for 24 h. After cleaning the residual solvent on the cotton fabric with deionized water, the sample was placed in an oven at 80 °C for 1 h and the contact angle was measured.

### 2.4 Oil–water separation test

The oil–water separation test was carried out in a self-made filter device with the superhydrophobic cotton fabric placed in the middle to serve as a filter layer. The oil–water mixture consists of 100 mL of oil colored with Sudan IV and 100 mL of water colored with methylene blue. Then the oil–water mixture was poured into the glass funnel and the oil quickly passed through the fabric into the conical flask due to gravity with the water being blocked. In order to prove the reusability of the

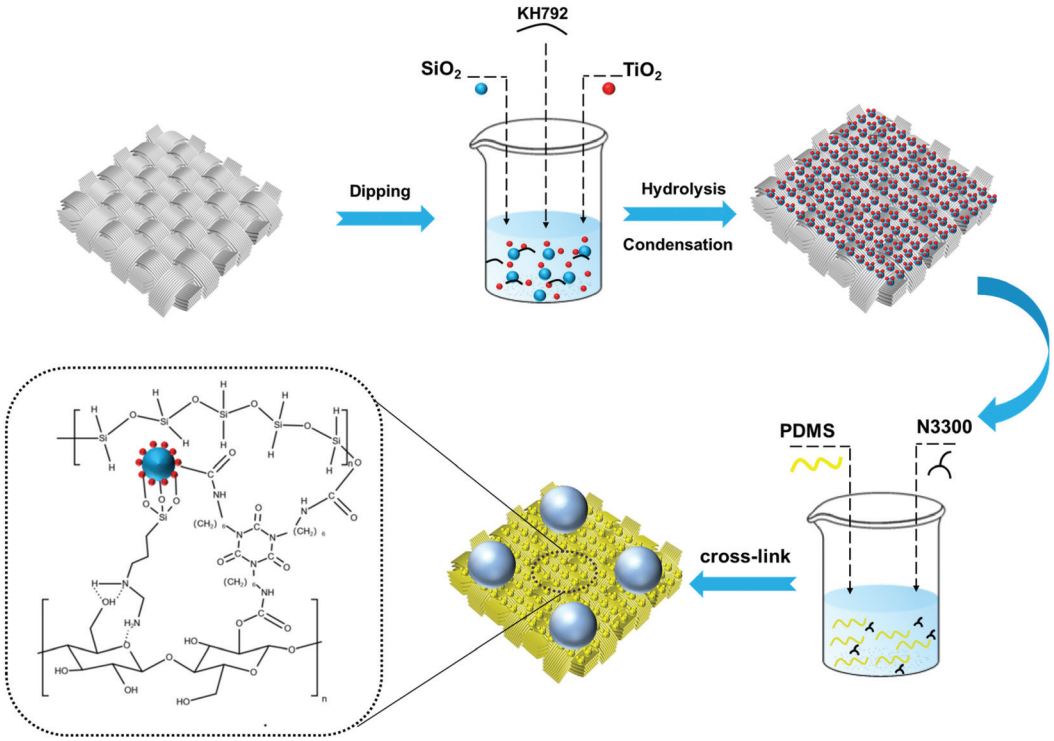


**Scheme 1** Schematic diagram of the preparation process of superhydrophobic cotton fabric.

superhydrophobic cotton fabric, this separation process was repeated for 30 cycles. After each cycle, the superhydrophobic cotton fabric was washed with ethanol and dried at 80 °C before the next cycle. After each oil–water separation was completed, the mass of the water in the glass funnel was weighed. And the oil–water separation efficiency $\eta_1$ was calculated by formula (1):

$$\eta_1 = \frac{m_1}{m_0} \times 100\% \quad (1)$$

where $m_1$ and $m_0$ are the mass of water after and before oil–water separation, respectively.

The oil–water separation flux ($J$) was calculated by formula (2):

$$J = \frac{V}{S \times T} \quad (2)$$

where $V$ represents the total volume of oil penetration, $S$ represents the effective cross-sectional area, and $T$ represents the time of oil penetration.

The oil-in-water emulsions were prepared by mixing water and toluene with the volume ratio of 50 : 1, where Span 80 (0.1 wt%) was used as the emulsifier. This mixture was vigorously ultrasonically dispersed for 1 h until a stable emulsion was formed.

### 2.5 Characterization

The surface morphology of the modified cotton fabric was characterized by field emission scanning electron microscopy (FESEM, JSM-7500F Japan). The elemental content on the surface of the cotton fabric was determined by an energy-dispersive spectrometer (X-Max N80) of SEM. The chemical compositions of pure and modified cotton fabric were examined by attenuated total reflectance Fourier transform infrared (ATR-FTIR, Nicolet 6700) spectroscopy. WCA was measured using a drop shape analyzer (DSA100S SN 30009557). The average value of the contact angle was obtained by measuring the contact angle three times at different positions on the cotton fabric with a water volume of 5 μL. UV-vis spectra were recorded by an ultraviolet visible near infrared spectrophotometer (Lambda 750 S). UV resistance stability was tested in a drawer light curing machine (1 kW, RXCT1000-300).

## 3. Results and discussion

### 3.1 Morphology and chemical analysis

The chemical compositions of the pure cotton fabric and the $SiO_2$–$TiO_2$/PDMS-coated superhydrophobic cotton fabric were analyzed by FTIR spectroscopy as shown in Fig. 1. In the FTIR spectrum of the pure cotton fabric (Fig. 1a), there were two prominent peaks at 3334 and 2898 $cm^{-1}$ corresponding to the stretching vibrations of –OH and –$CH_2$ groups, respectively.[43] Furthermore, a strong peak at 1028 $cm^{-1}$ was associated with the –OH bending vibration and the C–O–C stretching vibration. For the $SiO_2$–$TiO_2$/PDMS-coated superhydrophobic cotton fabric, a new peak appeared at 2964 $cm^{-1}$ attributed to the stretching vibration of the –$CH_3$ group from PDMS, indicating that PDMS was successfully bonded to the surface of the

 

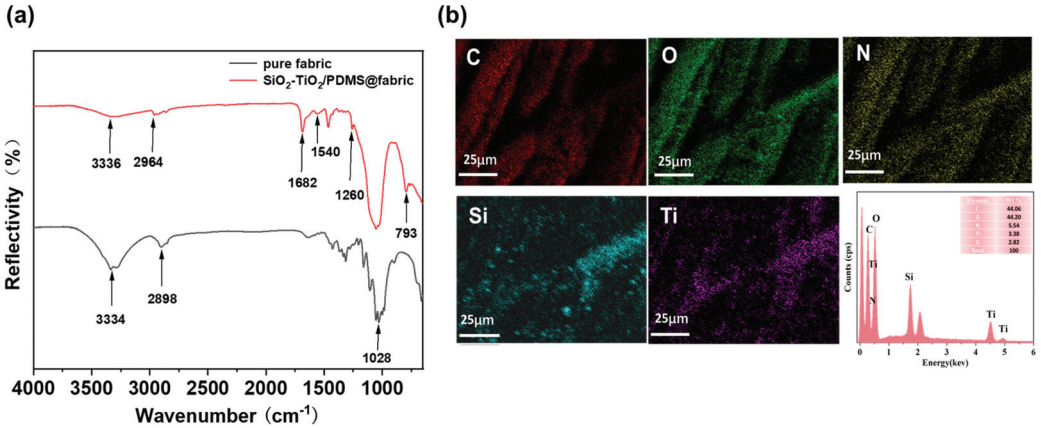


**Fig. 1** (a) FTIR spectra of pure cotton fabric and $SiO_2$–$TiO_2$/PDMS-coated superhydrophobic cotton fabric. (b) Element distribution map and curve of $SiO_2$–$TiO_2$/PDMS-coated superhydrophobic cotton fabric.

cotton fabric. The absorption peak at 1260 $cm^{-1}$ refers to the $-CH_3$ stretching vibration in $Si-CH_3$, also confirming the presence of the PDMS elastomer.[44] Moreover, a new typical peak at 793 $cm^{-1}$ had originated from the Si–O–Si symmetric stretching vibration from the Si–O–Si groups of PDMS.[45] Besides, the representative peaks of 1682 and 1540 $cm^{-1}$ were associated with the C═O stretching and N–H bending vibrations of the urethane bond, respectively, confirming the reaction of isocyanate and hydroxyl to produce a cross-linked network structure.[46] Meanwhile, a small absorption peak at 3336 $cm^{-1}$ belongs to –OH, which is obviously reduced, indicating that the surface hydroxyl groups were indeed bonded to the low-surface-energy PDMS through a cross-linked network. Furthermore, EDS was used to analyze the chemical composition of the cotton fabric surface. The pristine cotton fabric only contained two elements, C (53.35 wt%) and O (46.65 wt%), which were evenly distributed on the surface (Fig. S1a and b†). After functionalization of the cotton fabric, Si, Ti and N appeared in the EDS spectrum, and the corresponding contents are 2.82 wt%, 3.38 wt% and 5.54 wt%, respectively (Fig. 1b). As shown in Fig. 1b, elements Si and Ti were evenly distributed on the surface of the cotton fabric. The above results indicate that the $SiO_2$–$TiO_2$/PDMS-coated superhydrophobic cotton fabric was successfully prepared.

In order to study the effect of different proportions of micro-silica and nano-titanium dioxide on the surface morphology of superhydrophobic cotton fabrics, the morphologies of raw cotton, $SiO_2$/PDMS-coated cotton fabric, $TiO_2$/PDMS-coated cotton fabric, and $SiO_2$–$TiO_2$/PDMS-coated cotton fabric (the mass ratio of silicon dioxide to titanium dioxide was 1 : 1 based on 2% of the total mass) were characterized by SEM, as shown in Fig. 2. The surface of the pristine cotton fabric was smooth without any protrusions and textures (Fig. 2a). After being modified with micro-silica, the surface of the cotton fabric became rough with obvious protrusions (Fig. 2b). With the combination of this protruding structure and the low-surface-energy material, the air was trapped by this protruding structure, which forms a layer of air cushion,

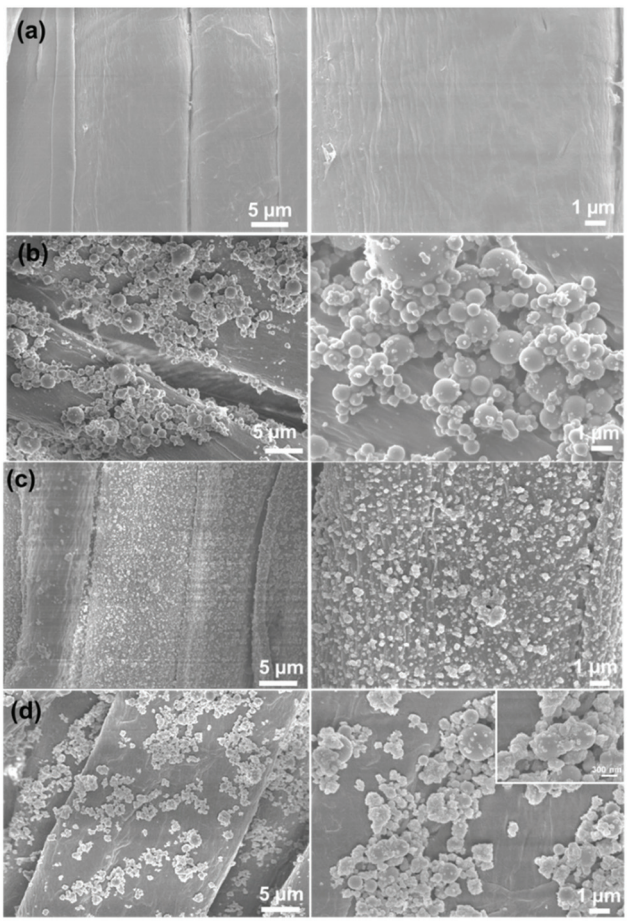


**Fig. 2** SEM images of (a) pristine cotton fabric, (b) $SiO_2$/PDMS-coated cotton fabric, (c) $TiO_2$/PDMS-coated cotton textile, and (d) $SiO_2$–$TiO_2$/PDMS-coated cotton fabric.

supporting water droplets, and the surface of the cotton fabric began to form superhydrophobicity with a WCA of 151.9° (Fig. 3a). For the $TiO_2$/PDMS-coated fabric, the surface was evenly covered with nano-sized titanium dioxide and the

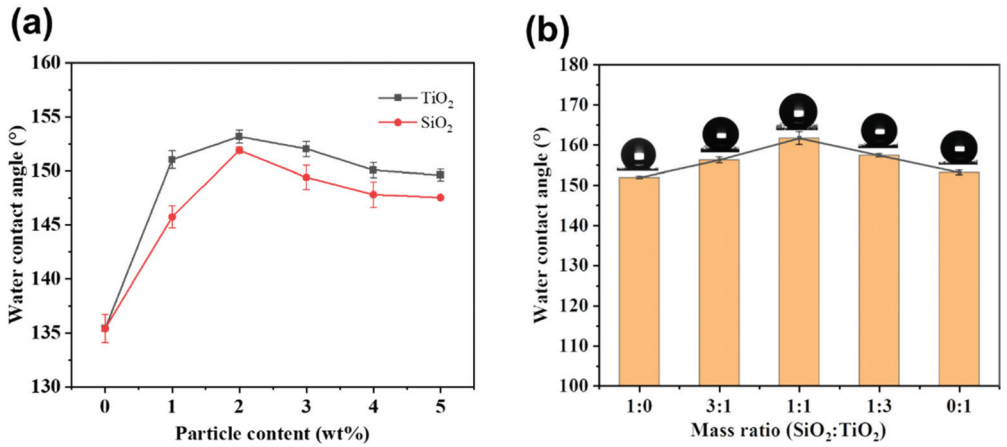


**Fig. 3** (a) The WCA of the modified cotton fabric prepared from different contents of $SiO_2$ and $TiO_2$ particles when the content of PDMS was 2 wt%. (b) The WCA of the modified cotton fabric prepared from different mass ratios of the two particles.

micro–nano structure of the surface was dependent on the agglomeration of nano-titanium dioxide (Fig. 2c). There the WCA was improved to 153.2° (Fig. 3a). In this $SiO_2$–$TiO_2$/PDMS, a more obvious hierarchical structure was formed and the protrusions were more evenly distributed on the surface of the cotton fabric, enabling a high WCA of 161.7° (Fig. 2d and 3b).

Fig. 3 illustrates the influence of the content of silica and titanium dioxide nanoparticles on the surface wettability of cotton fabrics. In general, both roughness and low surface energy determine the wettability of cotton fabric, and appropriate roughness combined with low surface energy could make the construction of superhydrophobic surfaces possible. Herein, the contact angle of water droplets was used as the main measure of the hydrophobicity of cotton fabrics. Fig. 3a displays the influence of $SiO_2$ and $TiO_2$ particle content on the wettability of cotton fabric when the content of PDMS was 2 wt%. The WCA of cotton fabric increased with the increase in silica and titanium dioxide nanoparticle content and the fabric reached the maximum hydrophobicity at 2% with a WCA of 151.9° and 153.2°, respectively, as shown in Fig. 3a. However, further increasing the content of silicon dioxide and titanium dioxide could lead to a decrease in the contact angle. For example, the contact angles of $SiO_2$/PDMS and $TiO_2$/PDMS coated fabric were 147.5° and 149.6°, respectively, when the particle content was 5%, indicating that excessive nanoparticles aggregated on the cotton fabric surface. In order to maximize the WCA, the content ratios of micro-silica and nano-titanium dioxide particles were studied based on the total content of 2 wt%. Fig. 3b illustrates the effect of different mass ratios of silicon dioxide and titanium dioxide on the WCA of cotton fabric. The WCA distinctly increased with different combinations of proportions, reaching the maximum of 161.7° when the mass ratio was 1 : 1. This increase might be due to the formation of a suitable micro–nano structure on the fabric surface with the combination of particles of different sizes.

The waterproof behavior of $SiO_2$–$TiO_2$/PDMS superhydrophobic cotton fabric in practice was investigated. Fig. 4a shows that water-based droplets in daily life were almost spherical on the superhydrophobic cotton fabric, indicating that the modi-

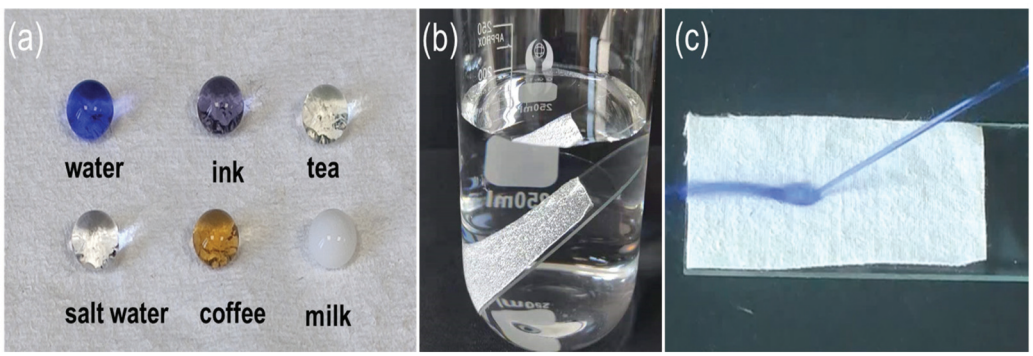


**Fig. 4** (a) Photographs of various water-based droplets on the modified cotton fabric, (b) silver mirror phenomenon when modified cotton fabric was immersed in water, and (c) jet water droplets bounced on the surface of modified cotton fabric.

 

fied cotton fabric was superhydrophobic. The functionalized superhydrophobic cotton fabric was immersed in water, and air trapped in the micro–nano structure was intuitively reflected. It is interesting that a bright silver mirror phenomenon was observed on the cotton fabric surface because air was trapped on the surface of the structure (Fig. 4b). The air effectively locked on the surface of the cotton fabric formed an air cushion and water droplets still bounced under the impact of high-speed water (Fig. 4c) which further demonstrated the good superhydrophobicity of the modified cotton fabric. It is known from the Cassie–Baxter equation that such excellent non-wetting properties are due to the low adhesion caused by the air cushion, which caused water droplets to easily roll off the surface of the cotton fabric.[47]

### 3.2 The UV protection performance of superhydrophobic cotton fabric

As shown in Fig. 5, the UV transmittance of cotton fabric decreased with the proportion of titanium dioxide increasing, which means that the UV protection effect of superhydrophobic cotton fabric was improved. The average transmittance values of UV-A (320–400 nm), UV-B (280–320 nm) and the whole UV range (200–400 nm) are given in Table 1. When the mass ratio of silicon dioxide to titanium dioxide was 1 : 1, the average transmittance decreased from 42.75%, 46.06%, and 45.36% for the original cotton fabric to 11.65%, 2.53%, and 6.85% for the UV-A region, UV-B region and the whole UV range, respectively, indicating that the UV protection performance increased by 85%. Furthermore, when all the nano-particles were titanium dioxide, the UV-A, UV-B, and whole UV range ultraviolet transmission was reduced to 2.16%, 0.15%, and 1.03%, respectively, showing excellent UV protection performance. The above results are due to the absorption and scattering of ultraviolet light by titanium dioxide, so that the superhydrophobic cotton fabric has good ultraviolet protection properties.[48] Combining the results of hydrophobicity and UV protection, the superhydrophobic cotton fabric made of equal mass of silica and titanium dioxide was used as the target of the subsequent tests.

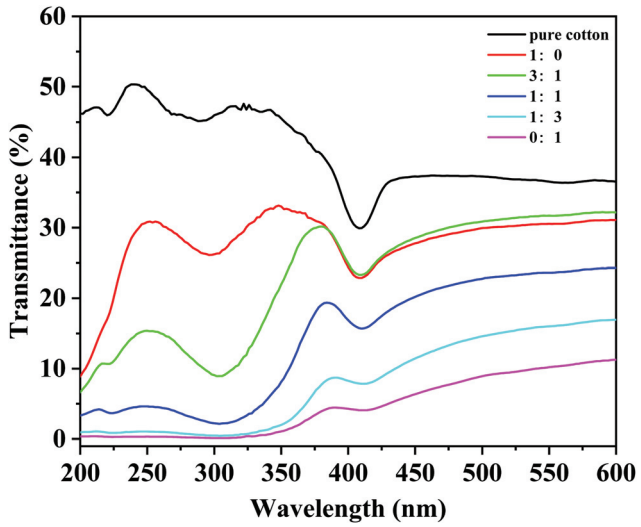


Fig. 5 UV transmittance of the pristine cotton fabric, and modified cotton fabric with different mass ratios of $SiO_2$ and $TiO_2$.

Table 1 UV-blocking properties of the untreated cotton and treated cotton fabric with different mass ratios of $SiO_2$ and $TiO_2$ particles

| Sample | Pristine fabric | 1 : 0 | 3 : 1 | 1 : 1 | 1 : 3 | 0 : 1 |
|---|---|---|---|---|---|---|
| UV-A (%) | 42.75 | 30.71 | 23.19 | 11.65 | 4.22 | 2.16 |
| UV-B (%) | 46.06 | 27.04 | 10.00 | 2.53 | 0.53 | 0.15 |
| Whole UV (%) | 45.36 | 27.22 | 16.36 | 6.85 | 2.20 | 1.03 |

### 3.3 Durability and chemical stability of $SiO_2$–$TiO_2$/PDMS-coated superhydrophobic cotton fabric

In practical applications, cotton fabrics are usually exposed to harsh external environments and will lose their superhydrophobicity due to external mechanical forces. Herein, the durability of the superhydrophobic cotton fabric was fully tested using tests such as sandpaper abrasion, washing test and UV resistance test. Fig. 6a displays how the sandpaper abrasion test was performed. Fig. 6b demonstrates that the change in the WCA was related to the sandpaper meshes and the number of cycles. After the functionalized cotton fabric was abraded by 2000 mesh sandpaper for 30 cycles, the surface still maintained superhydrophobicity with the WCA of 150.4° ± 0.35°. After 30 cycles with 800 mesh sandpaper, the WCA decreased to 142.4° ± 1.62° and the fabric lost its superhydrophobicity while still maintaining hydrophobicity. Fig. S2† shows the morphology of the superhydrophobic cotton fabric after 30 cycles of abrasion with 800 mesh sandpaper. Some cotton fibers on the surface were damaged and the roughness was severely damaged, leading to a significant decrease in the WCA. The WCA was between 161° and 150.3° when using 2000 mesh sandpaper, resulting in a small change compared with other meshes such as 800 and 1000 mesh sandpaper. It is confirmed that this superhydrophobic cotton fabric still had good mechanical strength due to the cross-linking network structure. Wash resistance stability was also tested by recording the change of WCA in different washing cycles, as shown in Fig. 6c. It indicates that the WCA changed slightly with increasing the number of wash cycles, and was maintained at 152.6° after 60 cycles, illustrating the excellent wash resistance of the modified superhydrophobic cotton fabric. Furthermore, the UV stability of the superhydrophobic cotton fabric was evaluated by measuring the contact angle after UV irradiation at different times. As shown in Fig. 6e, the WCA remained almost unchanged and reached 158.9° even after 24 h UV light irradiation, indicating good ability for withstanding ultraviolet light.

In addition, the chemical stability was evaluated by immersing the superhydrophobic cotton fabric in various corrosive liquids. As shown in the Fig. 6f, the WCA of the superhydro-

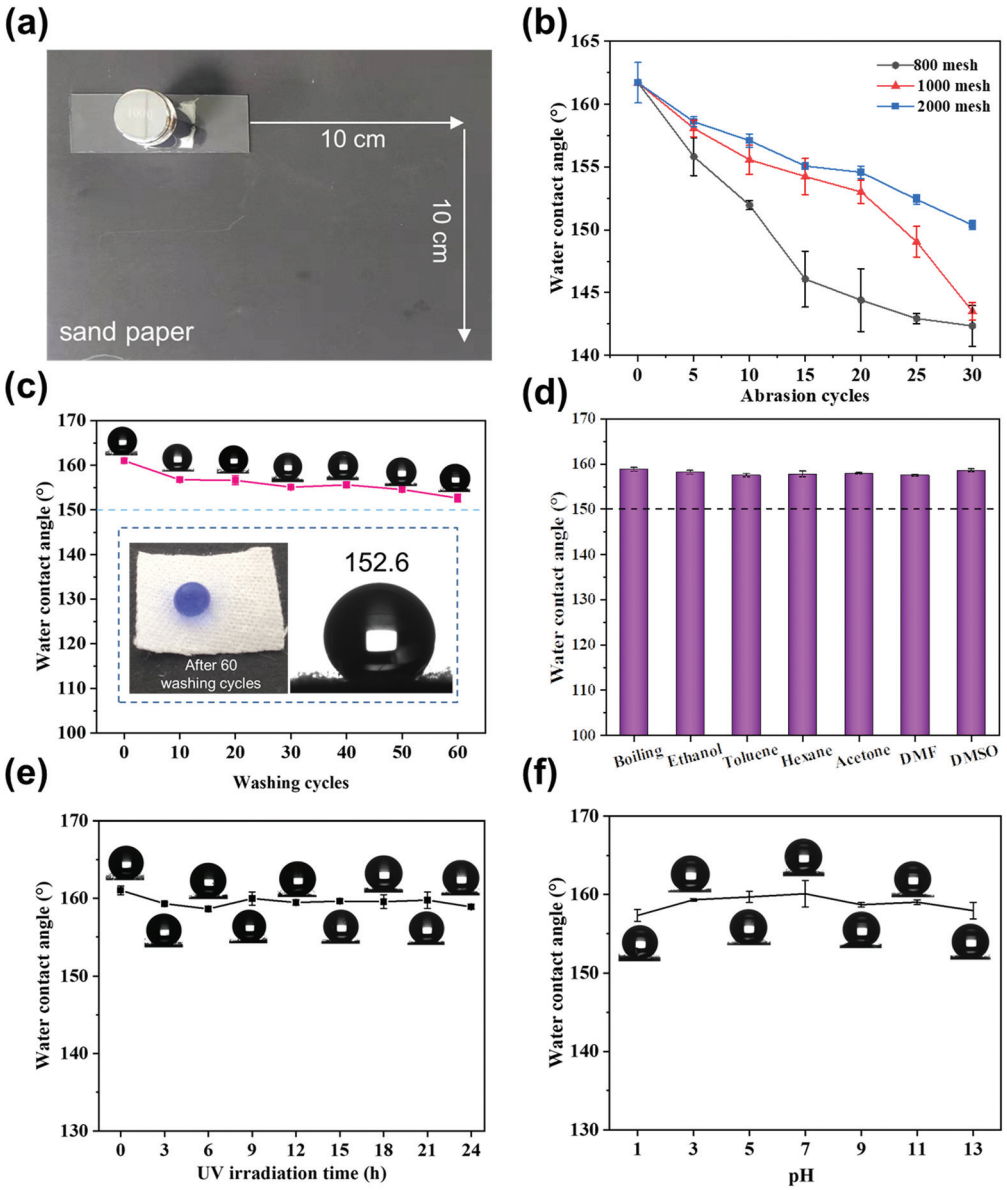


Fig. 6 (a) Photograph of abrasion resistance test. (b) The WCA variations of modified cotton fabric with abrasion cycles using different meshes. The influence of (c) washing (inset shows a water droplet lying on the surface of modified cotton fabric and the corresponding optical image of the static water droplets after 60 washing cycles), (d) various organic solvents/boiling water, (e) UV irradiation time, and (f) different pH values on the WCA of the superhydrophobic cotton fabric.

phobic cotton fabric immersed in pH = 1–13 aqueous solutions almost remained unchanged. Even after being immersed in various organic solvents and boiling water for 24 h, the WCA of the modified cotton fabric was still greater than 150° and maintained superhydrophobicity (Fig. 6d).

The excellent physical and chemical stability of the $SiO_2$–$TiO_2$/PDMS-coated superhydrophobic cotton fabric is attributed to the micro–nano rough structure and the cross-linking reaction of each component. When subjected to mechanical wear, the micro-silica protects the nano-titania so that the micro–nano structure is not damaged and the original superhydrophobic properties are well preserved. When immersed in corrosive liquid, this unique layered structure can trap a large amount of air, preventing the contact of corrosive liquids with the surface of the cotton fabric.

### 3.4 Self-cleaning and anti-fouling ability of superhydrophobic cotton fabric

In order to evaluate the self-cleaning effect, both pristine cotton fabric and modified cotton fabric were contaminated with sand and then placed on a glass slide (Fig. 7). The glass slide was placed on a Petri dish at an angle to allow water droplets dyed with methylene blue to roll off the surface of the cotton fabric. For the pristine cotton fabric, the sand was not

 

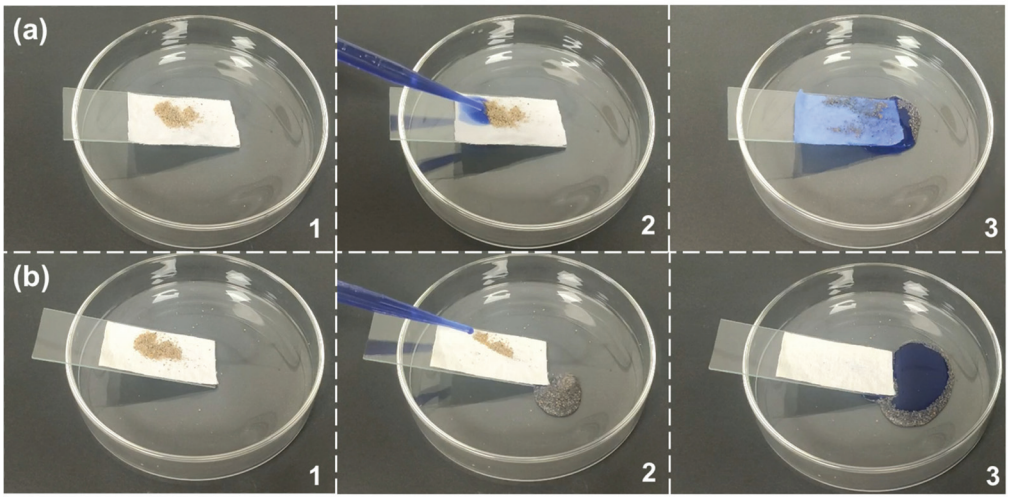


Fig. 7 The self-cleaning behavior of (a) pure cotton fabric and (b) $SiO_2$–$TiO_2$/PDMS coated superhydrophobic cotton fabric.

removed by water droplets from the cotton fabric which was wetted and contaminated by the dyed water (Fig. 7a). In contrast, the pollutants on the modified cotton fabric were immediately taken away by the falling water drops, leaving a clean surface (Fig. 7b). Therefore, this illustrates excellent self-cleaning ability of the modified cotton fabric.

### 3.5 Oil–water separation performance of $SiO_2$–$TiO_2$/PDMS-coated superhydrophobic cotton fabric

Because of the excellent selective wettability (superhydrophobic/superlipophilic), the prepared superhydrophobic cotton fabric could be used to absorb oil in an oil–water mixture. This

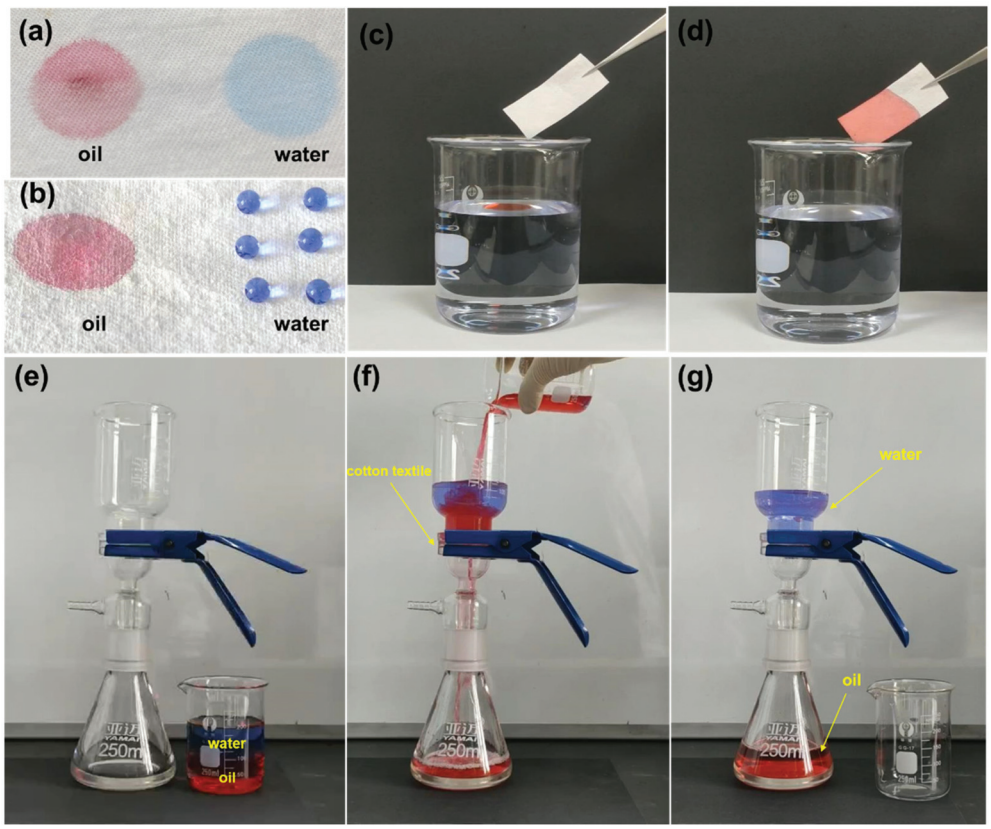


Fig. 8 Pictures of oil and water droplets on (a) the pure cotton fabric and (b) the $SiO_2$–$TiO_2$/PDMS-coated superhydrophobic cotton fabric. (c and d) Pictures of the absorbing process of *n*-hexane (dyed with Sudan IV) from water. (e–g) The dichloromethane–water mixture separation test of $SiO_2$–$TiO_2$/PDMS-coated superhydrophobic cotton fabric.

performance was initially confirmed by the wettability of the superhydrophobic cotton fabric to oil and water (Fig. 8a and b). It can be seen that the pure cotton fabric was superamphiphilic, and both oil and water were absorbed by the surface of the cotton fabric. However, only the oil was absorbed by the modified superhydrophobic cotton fabric and the water droplets formed a completely spherical shape on the surface. Furthermore, *n*-hexane colored with Sudan IV floating in water was absorbed by the modified superhydrophobic cotton fabric without leaving any red color in the beaker (Fig. 8c and d). The above results prove that the modified superhydrophobic cotton fabric exhibits lipophilic and hydrophobic properties, which are applied in the following oil–water separation experiment. The oil–water separation test was carried out with the dichloromethane–water mixture as an example. The separation process can be seen in Fig. 8e–g. The dichloromethane colored with Sudan IV driven by gravity quickly passed through the cotton fabric to the flask below, while the water colored with methylene blue was completely blocked. Therefore, there was no obvious red methylene chloride and blue water appearing in the funnel and bottom beaker after the separation process was completed, indicating the excellent oil–water separation efficiency of the prepared superhydrophobic cotton fabric.

After 30 separation cycles, the separation efficiency was slightly decreased and maintained at 99.3% while the separation flux was 20 279.34 L $m^{-2}$ $h^{-1}$, confirming the excellent oil–water separation ability of the prepared superhydrophobic cotton fabric for oil–water separation (Fig. 9a). The WCA of the superhydrophobic cotton fabric was measured after each oil–water separation to evaluate the reusability of the oil–water separation (Fig. S3†). The WCA of the superhydrophobic cotton fabric was still greater than 150° after 30 cycles, indicating that it had good oil–water separation ability and reusability. Moreover, other immiscible oil–water mixtures were also used for oil–water separation tests. As shown in Fig. 9b, all separation efficiencies were higher than 99%. Due to different viscosities of oils, the separation fluxes were very different and the corresponding oil fluxes were 20 762.62 ± 60.36, 14 140.91 ± 190.33, 12 760.91 ± 124.65, 11 843.60 ± 70.11, and 13 627.91 ± 84.26 L $m^{-2}$ $h^{-1}$ for dichloromethane, trichloromethane, dichloroethane, bromobenzene and carbon tetrachloride, respectively.

The oil–water separation mechanism of the $SiO_2$–$TiO_2$/PDMS-coated superhydrophobic cotton fabric was explained using oil and water wetting models (Fig. 10). Based on the Young–Laplace equation, the breakthrough pressure $\Delta p$ can be calculated as follows:

$$\Delta p = -\frac{2\gamma_l \cos\theta}{r_p} \quad (3)$$

where $\gamma_l$ is the surface tension of the liquid, $\theta$ is the contact angle of the liquid on cotton fabric, and $r_p$ represents the diameter of the holes between the fibers. For the prepared $SiO_2$–$TiO_2$/PDMS-coated superhydrophobic cotton fabric, the WCA was 161.7°, resulting in $\Delta p > 0$, which meant that water drops could not pass through the superhydrophobic cotton fabric (Fig. 10b).In contrast, the oil contact angle of the superhydro-

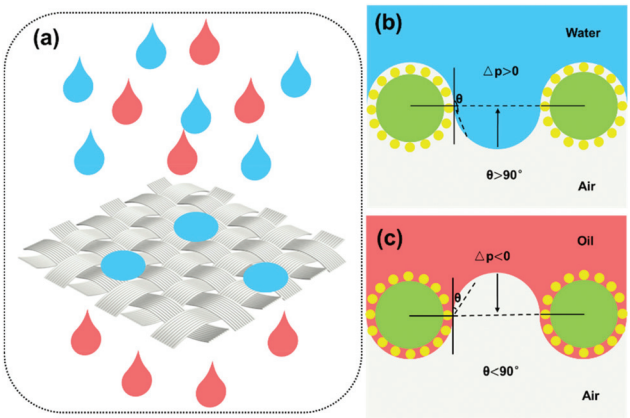


Fig. 10 (a) Schematic diagram of oil–water separation on $SiO_2$–$TiO_2$/PDMS-coated superhydrophobic cotton fabric. (b) Superhydrophobic cotton fabric can block water due to $\Delta p > 0$. (c) Superhydrophobic cotton fabric can absorb oil due to $\Delta p < 0$.

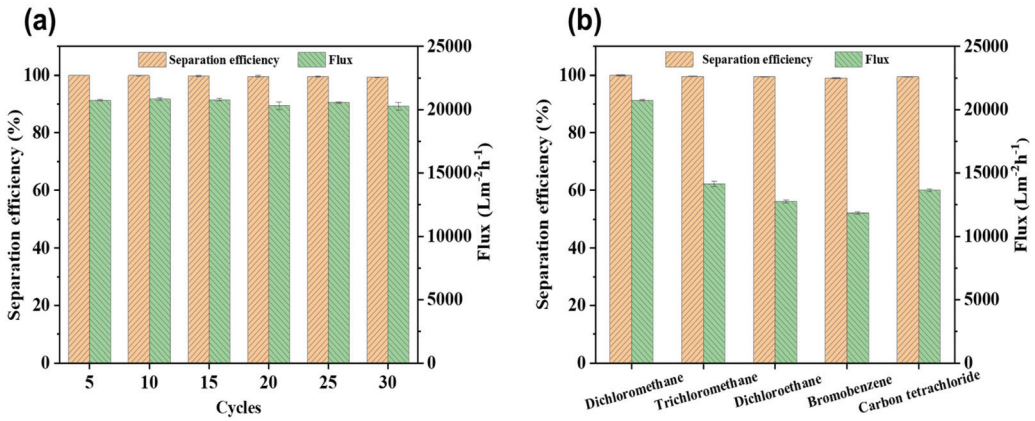


Fig. 9 (a) Separation efficiency and flux of a dichloromethane/water mixture during separation cycles. (b) Separation efficiency and flux for separating various immiscible oil/water mixtures.

phobic cotton fabric was ~0°, thus $\Delta p < 0$, indicating oil absorption by the superhydrophobic cotton fabric surface (Fig. 10c).

In real life, there are still oil-in-water emulsions which are more difficult to separate than immiscible oil–water mixtures. Herein, the surfactant Span 80 stabilized oil-in-water emulsions such as water–toluene. Fig. S4† shows the optical microscope images and digital photos of the oil-in-water emulsion before and after being separated by the superhydrophobic cotton fabric. It can be seen from the photos that the initial milky emulsion became clear and transparent after separation, indicating the successful separation of the oil–water emulsion. Furthermore, in the optical micrograph many small oil droplets filled the field of view before separation, while there were no visible oil droplets after separation.

## 4. Conclusion

In summary, a highly robust fluorine-free $SiO_2$–$TiO_2$/PDMS-coated superhydrophobic cotton fabric was prepared by a facile dip-coating method. A lotus-leaf-like rough surface was constructed by combining micro-silica and nano-titanium dioxide followed by PDMS modification. Due to low-surface-energy material and hierarchical rough surface, the $SiO_2$–$TiO_2$/PDMS-coated superhydrophobic cotton fabric shows excellent superhydrophobic properties with a WCA more than 161°. Moreover, the cross-linked structure of the surface endows good robustness and durability for sandpaper wear with 100 g weight loading for 30 cycles, 60 washing cycles and 24 h of UV radiation, as well as chemical stability in various organic solutions, boiling water and different pH solutions. Furthermore, the $SiO_2$–$TiO_2$/PDMS-coated superhydrophobic cotton fabric exhibits outstanding self-cleaning ability towards contaminants and UV protection performance compared with untreated cotton fabric. Additionally, high oil–water separation efficiency, and flux and good reusability were achieved towards an immiscible oil–water mixture and surfactant-stabilized oil-in-water emulsion. Therefore, such robust multifunctional $SiO_2$–$TiO_2$/PDMS-coated superhydrophobic cotton fabrics could be used in various fields such as water-proofing, self-cleaning and oil–water separation.

## Conflicts of interest

The authors declare no competing financial interest.

## Acknowledgements

This work was supported by the National Natural Science Foundation of China (21774098). This study was also financially supported by the Opening Project of State Key Laboratory of Polymer Materials Engineering (Sichuan University) (Grant No. sklpme2019-4-26) and the CRSRI Open Research Program (CKWV2021877/KY).

## References

1 C.-H. Xue, L.-L. Zhao, X.-J. Guo, Z.-Y. Ji, Y. Wu, S.-T. Jia and Q.-F. An, *Chem. Eng. J.*, 2020, **396**, 125231.
2 A. Biswas and N. R. Jana, *ACS Appl. Nano Mater.*, 2020, **4**, 877–885.
3 G. Huang, B. Lai, H. Xu, Y. Jin, L. Huo, Z. Li and Y. Deng, *Sep. Purif. Technol.*, 2021, **258**, 118063.
4 J. Chen, L. Yuan, C. Shi, C. Wu, Z. Long, H. Qiao, K. Wang and Q. H. Fan, *ACS Appl. Mater. Interfaces*, 2021, **13**, 18142–18151.
5 J. Zhang, L. Zhang and X. Gong, *Langmuir*, 2021, **37**, 6042–6051.
6 X. Lan, B. Zhang, J. Wang, X. Fan and J. Zhang, *Colloids Surf., A*, 2021, **624**, 126820.
7 C.-H. Xue, H.-G. Li, X.-J. Guo, Y.-R. Ding, B.-Y. Liu, Q.-F. An and Y. Zhou, *Chem. Eng. J.*, 2021, **424**, 130553.
8 T. Zhu, Y. Cheng, J. Huang, J. Xiong, M. Ge, J. Mao, Z. Liu, X. Dong, Z. Chen and Y. Lai, *Chem. Eng. J.*, 2020, **399**, 125746.
9 Y. Shen, K. Li, H. Chen, Z. Wu and Z. Wang, *Chem. Eng. J.*, 2021, **413**, 127455.
10 R. Zhu, M. Liu, Y. Hou, L. Zhang, M. Li, D. Wang, D. Wang and S. Fu, *ACS Appl. Mater. Interfaces*, 2020, **12**, 50113–50125.
11 W. Rong, H. Zhang, Z. Mao, L. Chen and X. Liu, *Colloids Surf., A*, 2021, **622**, 126712.
12 D. Daksa Ejeta, C.-F. Wang, S.-W. Kuo, J.-K. Chen, H.-C. Tsai, W.-S. Hung, C.-C. Hu and J.-Y. Lai, *Chem. Eng. J.*, 2020, **402**, 126289.
13 Í. G. M. da Silva, E. F. Lucas and R. Advincula, *Sep. Purif. Technol.*, 2022, **278**, 119365.
14 L. Shen, X. Wang, Z. Zhang, X. Jin, M. Jiang and J. Zhang, *ACS Appl. Mater. Interfaces*, 2021, **13**, 14653–14661.
15 H. Li, P. Mu, J. Li and Q. Wang, *J. Mater. Chem. A*, 2021, **9**, 4167–4175.
16 L. Zhong, H. Tao and X. Gong, *Langmuir*, 2021, **37**, 6765–6775.
17 J. Zhang, L. Zhang and X. Gong, *Soft Matter*, 2021, **17**, 6542–6551.
18 M. Wu, G. Shi, W. Liu, Y. Long, P. Mu and J. Li, *ACS Appl. Mater. Interfaces*, 2021, **13**, 14759–14767.
19 H. Yu, M. Wu, G. Duan and X. Gong, *Nanoscale*, 2022, **14**, 1296–1309.
20 W. Barthlott and C. Neinhuis, *Planta*, 1997, **202**, 1–8.
21 R. N. Wenzel, *Ind. Eng. Chem.*, 1936, **28**, 988–994.
22 A. B. D. Cassie and S. Baxter, *Trans. Faraday Soc.*, 1944, **40**, 546–551.
23 W. Guo, X. Wang, J. Huang, Y. Zhou, W. Cai, J. Wang, L. Song and Y. Hu, *Chem. Eng. J.*, 2020, **398**, 125661.
24 D. W. Wei, H. Wei, A. C. Gauthier, J. Song, Y. Jin and H. Xiao, *J. Bioresour. Bioprod.*, 2020, **5**, 1–15.
25 W. Ma, Y. Ding, Y. Li, S. Gao, Z. Jiang, J. Cui, C. Huang and G. Fu, *J. Membr. Sci.*, 2021, **634**, 119402.
26 Y. Fu, B. Jin, Q. Zhang, X. Zhan and F. Chen, *ACS Appl. Mater. Interfaces*, 2017, **9**, 30161–30170.

27 W. Kong, F. Li, Y. Pan and X. Zhao, *ACS Appl. Mater. Interfaces*, 2021, **13**, 35142–35152.
28 V. C. Mai, S. Hou, P. R. Pillai, T. T. Lim and H. Duan, *ACS Nano*, 2021, **15**, 6977–6986.
29 W. Rao, J. Shi, C. Yu, H.-B. Zhao and Y.-Z. Wang, *Chem. Eng. J.*, 2021, **424**, 130556.
30 X. Zhang, P. Zhang, M. Lu, D. Qi, P. Muller-Buschbaum and Q. Zhong, *ACS Appl. Mater. Interfaces*, 2021, **13**, 27372–27381.
31 F. Guan, Z. Song, F. Xin, H. Wang, D. Yu, G. Li and W. Liu, *J. Bioresour. Bioprod.*, 2020, **5**, 37–43.
32 X. Li, X. Wang, Y. Yuan, M. Wu, Q. Wu, J. Liu, J. Yang and J. Zhang, *Eur. Polym. J.*, 2021, **159**, 110729.
33 X. Zhou, Z. Zhang, X. Xu, F. Guo, X. Zhu, X. Men and B. Ge, *ACS Appl. Mater. Interfaces*, 2013, **5**, 7208–7214.
34 Y. Sun, J. Huang and Z. Guo, *Langmuir*, 2020, **36**, 5802–5808.
35 Q. Shang, J. Cheng, C. Liu, L. Hu, C. Bo, Y. Hu, X. Yang, X. Ren, Y. Zhou and W. Lei, *Prog. Org. Coat.*, 2021, **158**, 106343.
36 Y. N. Gao, Y. Wang, T. N. Yue, Y. X. Weng and M. Wang, *J. Colloid Interface Sci.*, 2021, **582**, 112–123.
37 S. K. Lahiri, P. Zhang, C. Zhang and L. Liu, *ACS Appl. Mater. Interfaces*, 2019, **11**, 10262–10275.
38 S. Pal, S. Mondal, P. Pal, A. Das, S. Pramanik and J. Maity, *Colloid Interface Sci. Commun.*, 2021, **44**, 100469.
39 Q. Shang, L. Hu, X. Yang, Y. Hu, C. Bo, Z. Pan, X. Ren, C. Liu and Y. Zhou, *Prog. Org. Coat.*, 2021, **154**, 106191.
40 X. Chen, Q. Zhou, Y. Zhang, J. Zhao, B. Yan, S. Tang, T. Xing and G. Chen, *Colloids Surf., A*, 2020, **586**, 124175.
41 Q. Shang, C. Liu, J. Chen, X. Yang, Y. Hu, L. Hu, Y. Zhou and X. Ren, *ACS Sustainable Chem. Eng.*, 2020, **8**, 7423–7435.
42 L. Xu, Y. Liu, X. Yuan, J. Wan, L. Wang, H. Pan and Y. Shen, *Cellulose*, 2020, **27**, 9005–9026.
43 C. Chung, M. Lee and E. Choe, *Carbohydr. Polym.*, 2004, **58**, 417–420.
44 H. Liu, L. Yang, Y. Zhan, J. Lan, J. Shang, M. Zhou and S. Lin, *Cellulose*, 2021, **28**, 1715–1729.
45 E. Pakdel, H. Zhao, J. Wang, B. Tang, R. J. Varley and X. Wang, *Cellulose*, 2021, **565**, 8807–8820.
46 X. Liu, X. Liu, W. Li, Y. Ru, Y. Li, A. Sun and L. Wei, *Chem. Eng. J.*, 2021, **410**, 128300.
47 Y. Sun and Z. Guo, *Nanoscale Horiz.*, 2019, **4**, 52–76.
48 J. Y. Huang, S. H. Li, M. Z. Ge, L. N. Wang, T. L. Xing, G. Q. Chen, X. F. Liu, S. S. Al-Deyab, K. Q. Zhang, T. Chen and Y. K. Lai, *J. Mater. Chem. A*, 2015, **3**, 2825–2832.